



**HAL**  
open science

## Determination of the shear modulus of colloidal solids with high accuracy

T. Palberg, J. Kottal, T. Loga, H. Hecht, E. Simnacher, F. Falcoz, P. Leiderer

► **To cite this version:**

T. Palberg, J. Kottal, T. Loga, H. Hecht, E. Simnacher, et al.. Determination of the shear modulus of colloidal solids with high accuracy. *Journal de Physique III*, 1994, 4 (3), pp.457-471. 10.1051/jp3:1994139 . jpa-00249116

**HAL Id: jpa-00249116**

**<https://hal.science/jpa-00249116v1>**

Submitted on 4 Feb 2008

**HAL** is a multi-disciplinary open access archive for the deposit and dissemination of scientific research documents, whether they are published or not. The documents may come from teaching and research institutions in France or abroad, or from public or private research centers.

L'archive ouverte pluridisciplinaire **HAL**, est destinée au dépôt et à la diffusion de documents scientifiques de niveau recherche, publiés ou non, émanant des établissements d'enseignement et de recherche français ou étrangers, des laboratoires publics ou privés.

Classification

Physics Abstracts

82.70 — 46.30R — 81.40

## Determination of the shear modulus of colloidal solids with high accuracy

T. Palberg, J. Kottal, T. Loga, H. Hecht, E. Simnacher, F. Falcoz and P. Leiderer

Fakultät für Physik, Universität Konstanz, D-78434 Konstanz, Germany

(Received 23 March 1993, revised 25 November 1993, accepted 14 December 1993)

**Abstract.** — We report high accuracy and precision measurements of the shear modulus of colloidal solids formed from monodisperse charged latex spheres contained in an aqueous electrolyte. Standard preparational techniques as well as a recently reported advanced deionization method are applied to prepare transparent, bcc-crystalline samples at precisely controlled low volume fractions  $\Phi = 0.003$  and salt concentrations  $c_s \leq 2 \mu\text{mol l}^{-1}$ . The experimental parameters are found to be extremely stable if certain precautions are taken. At constant experimental conditions samples of different morphologies are prepared *via* controlled solidification and further shear processing. Their structure, texture and morphology are analysed by various static light scattering methods. A new, non destructive, time resolved static light scattering technique is used to detect the resonant torsional vibrations excited within a cylindrical sample. Shear moduli in dependence on the concentration of excess electrolyte are calculated from the resonance spectra and compared for several sample morphologies. For the first time a sufficiently high resolution is achieved to clearly discriminate between the influence of the morphology of the sample and of the experimental parameters. We discuss the possible applications of this new approach of high accuracy shear modulus measurements in colloidal crystals to a wide range of interesting experiments.

### Introduction.

Under certain conditions of low concentration of excess electrolyte suspensions of monodisperse, charged latex spheres spontaneously form ordered interparticle structures, so-called colloidal fluids, glasses and crystals [1-3]. Such soft matter phases show a number of structural analogies to atomically condensed matter [4]. They furthermore exhibit many features specific to colloidal systems, such as Brownian dynamics or the accessibility on an interparticle scale by light scattering and microscopic techniques [5].

In particular, the elastic and plastic response of colloidal solids subjected to external shearing fields has attracted considerable interest over the last few years. The extensive experimental and theoretical work [6-13] was motivated by the long term perspectives to gain access to very general concepts for the deformation and processing of crystalline material on a microscopic scale [15]. Due to the low volume fractions  $\Phi \approx 0.01$  of charge stabilized colloidal crystals the observed elastic moduli are in the range of only a few ten Pa. So are the yield stresses. Colloidal crystals are therefore extremely fragile objects which can easily be deformed or even shear molten simply by shaking the sample [16-20].

At low shear rates the structure, texture and morphology of an individual sample may be modified by a number of processes including controlled solidification, annealing and wearing under shear. E.g. shear processing leads to self organized, checkerboard-like or other complex texture patterns [16, 17]. In flow through geometries at moderate suspension velocities the resonant coupling of a stick-slip process between wall and colloidal crystal to an internal shear vibration of the colloidal solid was observed. At higher flow velocities the sample underwent a phase transition to a shear molten state [18]. Quantitative examinations in a Couette flow show a succession of different phases as a function of the applied shear rate [19, 20]. Clearly, the explanation of such non equilibrium phenomena will rely on the knowledge of the elastic properties of the samples. These, in turn, are related to the experimental parameters but moreover to structural, textural and morphological details.

Already in 1977 the bulk modulus of a polycrystalline material was determined from the gravitational compression of a colloidal solid [6]. In a series of pioneering experiments several authors determined the general dependence of the shear modulus  $G$  on the experimental parameters volume fraction  $\Phi$  and concentration of excess electrolyte  $c$ , [7-10].  $G$  was found to decrease with increasing salt concentration and decreasing volume fraction.

Since most of the samples investigated were opaque, only the outermost regions next to the cell wall were subjected to structural investigations. Thus, important informations about morphological details — like homogeneity of the sample, grain size distribution and the degree, respectively direction of orientation—were not available. Therefore the samples had to be assumed to have an unoriented polycrystalline morphology. Systematic deviations between calculated and experimentally measured shear moduli remained unexplained ; e.g. the stronger than predicted increase of  $G$  with increasing volume fraction [10].

Determination of the influence of the morphology faces three major technical difficulties. Firstly the preparation of transparent samples (low volume fraction  $\Phi \approx 0.004$ ) under precise control and stabilization of the experimental conditions. In particular, contamination with air born  $\text{CO}_2$  has to be avoided. Secondly the characterization of the morphology of the sample and thirdly the accurate detection of the shear modulus. Since the shear moduli and yield stresses of colloidal systems with volume fractions below  $\Phi \leq 0.004$  are in the sub-Pascal range, non-destructive light scattering methods have to be applied. The use of mechanical detection [10] is severely limited. The analysis of kossel lines [7] is restricted to opaque samples and cannot be applied, too.

We therefore here report the combination of a recently described advanced preparational technique [21] with a morphological analysis by static light scattering and a novel detection scheme for resonant shear vibrations. All of these are particularly suited for the study of low volume fraction, low salt concentration colloidal solids. This combination is compared to other approaches with respect to accuracy and reproducibility.

We first give a short outline of the theoretical background. We then introduce the experimental procedures which are thoroughly tested to ensure stable experimental parameters, accurate shear modulus measurements and reproducible sample preparation. We then measure the shear modulus of samples of different morphologies in dependence on the salt concentration. The interpretation of the results and possible applications of the described approach will be considered in some detail in the discussion section.

### Theoretical.

The interpretation of the results relies on the description of the pair potential of interaction between the particles, on its relation to the elastic properties of the sample and on the evaluation of detected resonance frequencies to the shear modulus.

In the limit of low salt concentrations  $c_s$  and volume fractions  $\Phi = 4/3 \pi a^3 n_p$  (where  $n_p$  is the particle density) the energy of interaction between two colloidal spheres of equal radius  $a$  at a separation  $r$  is may be described in terms of the modified DeJarguin-Laudau-Verwey-Overbeek approximation (MDA) [9]. In this description the true charge number  $Z$  and the Debye screening parameter  $\kappa$  are replaced by the somewhat smaller renormalized values  $Z^*$ , respectively  $\kappa^*$  [22-24]. The MDA is given by :

$$V(r) = \frac{Z^{*2} e^2}{4 \pi \epsilon} \left( \frac{\exp(\kappa^* a)}{(1 + \kappa^* a)} \right)^2 \frac{\exp(-\kappa^* r)}{r} \quad (1)$$

with  $\kappa^*$  depending on the charge and concentration of particles as well as on the number density  $n_s$  of all small ions other than  $H^+$  counter ions :

$$\kappa^{*2} = \frac{e^2}{\epsilon k_B T} (n_p Z^* + n_s). \quad (2)$$

Here  $\epsilon = \epsilon_0 \epsilon_r$  is the dielectric permittivity of the suspending medium  $k_B$  the Boltzmann constant,  $T$  the temperature and  $e$  is the elementary charge. Due to the high charge numbers and the low volume fractions of the suspensions examined here we may safely neglect van der Waals, respectively hydrodynamic interactions.

The derivation of values for the shear modulus  $G$  in close analogy to the shear modulus predictions for atomic solids includes nearest neighbour interactions and assumes the volume of noncrystalline material in grain boundaries to be negligibly small [9]. For such conditions the shear modulus  $G$  of a polycrystalline sample may be described as :

$$G = f_s f_A n_p \frac{d^2 U(d_{NN})}{d d_{NN}^2} \quad (3)$$

with  $f_s$  being a factor depending on the structure (4/9 for bcc and 1/4 for fcc);  $d_{NN}$  is the shortest inter-particle spacing. The known analytical factor  $f_A$  results from taking the average of the anisotropic elastic properties of the single crystallites contained in the sample volume. For a sample of equally sized cubic crystallites with no preferred orientation it is 0.6 if homogeneous strain is assumed and 0.4 if the averaging is taken of homogeneously stressed crystals [9, 14]. For most atomic solids, however, a value of  $f_A = 0.5$  is found empirically [15].

In the case of oriented polycrystalline or single crystalline material the anisotropic elastic properties are not averaged out ; consequently  $f_A$  may take largely different values depending on the relative orientation between the crystal axes and the direction of applied shear. In general for a bcc crystal  $G$  is largest for shear along a (100) plane in [100] direction and minimal for shear along a (110) plane in [111] direction. For charge stabilized colloidal solids these values have been computed and tabulated for single crystals together with averaged values for unoriented polycrystalline materials [14]. Although as yet no predictions are available for oriented polycrystalline material, it is easy to see that for increasing texturing  $G$  will approach the single crystal values of the respective relative orientations.

Any colloidal solid exhibiting a finite  $G$  may be excited to low frequency torsional resonances ; (due to the presence of the viscous suspending medium the high frequency vibrations are overdamped). For a cylindrical resonator cell of height  $H$  and radius  $R$ , i.e. for an aspect ratio  $\alpha = R/H$  with the colloidal solid sticking to both the wall and the bottom of the half filled resonator cell, Joanny solved the equation of motion to yield the resonance frequencies as [12] :

$$\omega = \frac{1}{R} \left[ \frac{G}{\rho} \left( \mu_j^2 + \left( i + \frac{1}{2} \right)^2 \pi^2 \alpha^2 \right) \right]. \quad (4)$$

Here  $\rho$  is the sample density,  $\mu_j$  denotes the zeros of spherical Bessel functions of first order with  $j = 1, 2, 3, \dots$  and the number of nodes of the vertical standing wave within the height  $H$  is given by  $i = 0, 1, 2, \dots$ . Explicit hydrodynamic calculations yield the same result in the limit of small particle elongations and small relative velocities between the particles and the suspending medium [13]. The same solution holds for a cylinder of height  $2H$  with the colloidal solid sticking also to the top of the resonator cell. The shear modulus is then derived from the measured resonance frequencies as :

$$G = \frac{R^2 \rho^2 \omega^2}{\mu_{ij}^2 + (i + 1/2)^2 \pi^2 \alpha^2}. \quad (5)$$

### Experimental procedures.

**SAMPLE PREPARATION.** — The particles used were commercially available [Lot 2011 M9R, Seradyn, In., USA] polystyrene spheres of diameter  $\sigma = 102$  nm and a titrated number of  $N = 950 \pm 20$  strongly acidic surface groups. To deionize the suspensions mixed bed ion exchange resin [MB1, SERVA, FRG] was used. All salt solutions were p.a. grade and handled under inert gas ; dilution was done with water of a maximum conductivity of  $85 \text{ nS cm}^{-1}$  at  $20^\circ\text{C}$ .

Two procedures are available to deionize the sample : « standing preparation » (SP) and « continuous deionization » (CD) [21]. Standing preparation refers to the standard technique of introducing a small amount of ion exchange resin into the sample cell containing the suspension. A fine mesh covering the resin beads assures the flat lower boundary needed for the experiment. After a few weeks the sample crystallizes, but the procedure may be accelerated by occasional mild agitation. The actual state of the deionization process is not monitored directly. Great care has to be taken to completely seal the sample cell against contamination with air-borne  $\text{CO}_2$  in order to avoid salt gradient induced inhomogeneities [25]. Because of that any free air-suspension interface has to be avoided the sample cells have to remain unopened. SP therefore produces completely deionized samples of fixed volume fraction.

As details of CD are given elsewhere [21] we only summarize here the basic features. The suspension is peristaltically pumped through a teflon tubing system connecting an ion exchanger cell, a conductivity cell and the actual measuring cell. No free gas-suspension interface is present in the measuring cell. A bypass of the ion exchanger cell and a reservoir under inert gas allows for the subsequent addition of salty suspensions to the completely deionized sample. The actual salt concentration is monitored *in situ via* conductivity. CD was shown to be fast, reproducible and accurate with no residual gradients in particle and salt concentrations. The uncertainties in volume fraction  $\Phi$  and salt concentration  $c_s$  are below 1 %, respectively 2 % at  $\Phi \leq 0.004$  and  $c_s \leq 10^{-6}$  [21]. CD leaves the sample in a shear molten state that readily solidifies. The morphology and texture are influenced *via* shear processing during crystal growth or after complete solidification.

Both methods are easily incorporated into the set-up for time resolved static light scattering. The main results nevertheless were measured after preparation with CD. To employ the mirror method of detection the sample cell is only half-filled and a free upper surface is present.

**DETECTION OF RESONANT SHEAR MODES BY LIGHT SCATTERING.** — We would first like to note, that there are no principal limitations in the optical detection of resonant shear modes to a specific sample geometry nor to a special method of exciting resonant shear vibrations. The method has indeed been applied also to resonant modes excited in single crystals [18] under

flow through a rectangular cell or in polycrystalline material subjected to alternating, inhomogeneous electric fields [26]. However, in this article we will restrict ourselves to outlining the basic principles for a cylindrical resonator geometry and mechanical oscillations of the sample cell.

The experimental situation is sketched in figure 1 with the  $J_{10}$  mode shown in the middle of the resonator filled with a colloidal solid. The resonator cell is held by ball bearings and is excited mechanically by an excentrically coupled loudspeaker DR driven by a frequency generator FG. A laser beam is incident on a small crystallite C in the cell centre and scattered upon a position sensitive photo detector D under an angle  $\Theta_{Br}$  satisfying a Bragg condition.

Upon periodic torsional vibration the intensity of Bragg scattered light will contain terms of motion of the crystallite in and out of the beam as well as terms of rotation of the crystallite to and from the orientation favourable for Bragg reflection. In the limit of very tiny displacements the latter contributions can be neglected and the intensity stays practically constant. The Bragg angle, however, is shifted periodically with the variation of lattice spacings:  $\Theta_{Br}(t) = 2 \sin^{-1}(\lambda/2 nd_{hkl}(t))$ ; where  $\lambda$  is the wavelength of light and  $d_{hkl}(t)$  denotes the respective spacing of  $(hkl)$  crystal planes. For small elongations the sinusoidal variation of lattice spacings is transformed into equally sinusoidal variation of  $\Theta_{Br}$ . The response signal of the position sensitive detector is fed into a lock-in-amplifier LI or a frequency analyser. The generated resonance spectrum is further processed and evaluated with a computer.

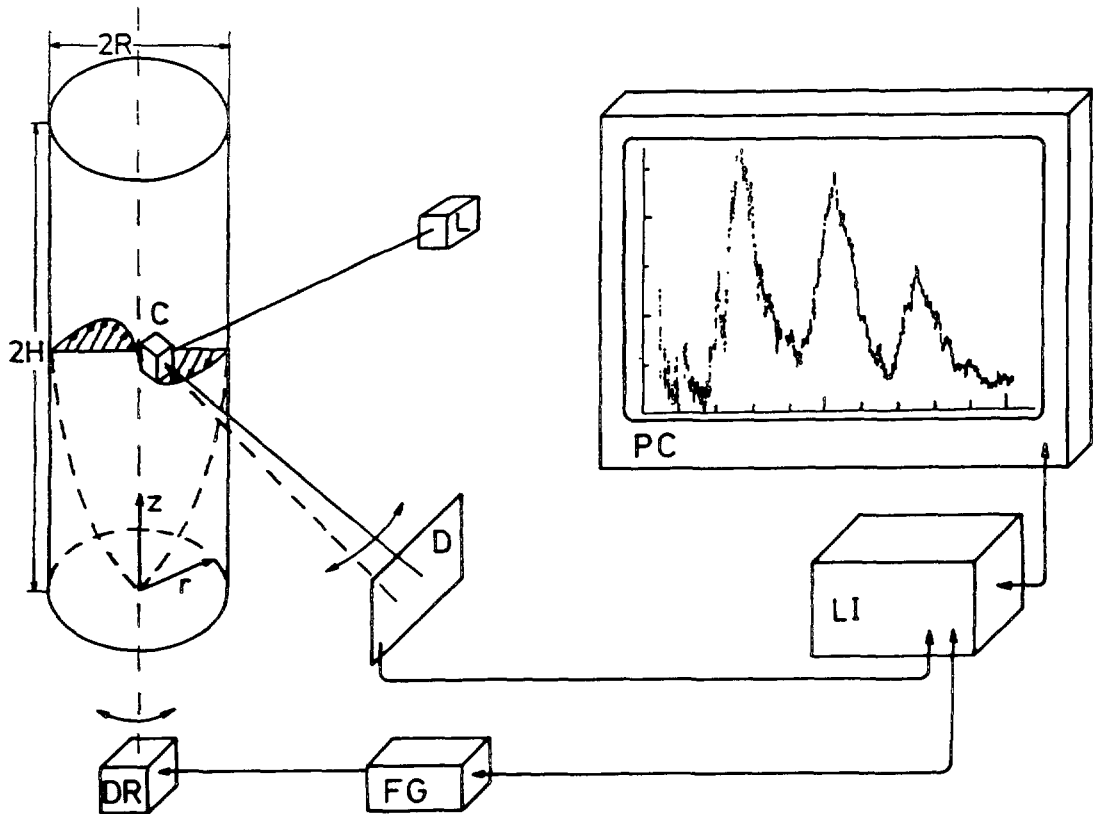


Fig. 1. — Experimental set-up: L: laser; C: crystal oriented under Bragg condition; D: position sensitive detector; DR: drive; FG: frequency generator; LI: lock-in amplifier; PC: computer.

The sample cell is placed in a cylindrical thermostatted index match bath centred on a goniometer. This serves as a cylindrical lens focussing all light scattered under a given angle  $\theta$  from arbitrary points in the scattering volume onto a point lying on a radius of 26.5 cm. A photomultiplier arrangement allows for the detection of the equilibrium static structure factor for both crystalline and amorphous samples *via* a Debye-Scherrer technique. For this purpose we replace the rocking drive by a motor continuously turning the sample. Thus, also particle concentrations  $n_p$  may be measured *in situ*. For all samples a fixed volume fraction was adjusted of  $\Phi = 0.0028$  corresponding to  $n_p = 5.40 \times 10^{18} \text{ m}^{-3}$ .

MIRROR METHOD. — We further use a second detection scheme already successfully employed by other authors [9, 14]. The sample is prepared by SP or CD having a free upper inert gas-suspension interface. A small mirror is centred on this surface. It reflects a laser beam onto the position sensitive detector. Data analysis is performed as before. The collection of reproducible data with this detection scheme requires a lot of patience, since actually a lot of care has to be taken in avoiding contamination with  $\text{CO}_2$ , while handling the mirror under the inert gas atmosphere. In the presence of ion exchange resin this in turn might lead to gradients in salt concentration followed by gradients in particle concentrations [25]. For CD in- and outlets have to be at the cell bottom, which often induces insufficient mixing of the suspension, particularly close to the mirror. In both cases additional mixing using a magnetic stirrer was tried but led to insufficiently defined cell geometry and irreproducible shifts in the resonance frequencies. For some of the experiments we worked under air to truly reproduce other authors' experimental conditions.

DETERMINATION OF MORPHOLOGY AND TEXTURE. — We here investigate samples ranging from purely unoriented to strongly oriented polycrystalline material. In addition mixed morphologies are prepared showing a polycrystalline core surrounded by a monolithic crystal. As a detailed investigation of the possible variety of sample morphologies and textures is still in progress, we here only give a short sketch of the basic experimental procedures employed to determine the sample structure, the crystallite sizes and their preferred orientations.

The equilibrium structure factors are measured with a Debye-Scherrer like technique using the above mentioned static light scattering set-up. In order to determine the morphological details the photomultiplier arrangement is replaced by a cylindrical translucent screen. This is also placed at a distance of 26.5 cm from the cell center, i.e. at the focus of the index match bath. On this screen the Debye-Scherrer rings of the (110) and of higher order reflections are visible for polycrystalline bcc samples.

The sample is slowly turned around its  $z$ -axis to achieve optimum averaging. The screen is observed by a video camera. The video frames are further processed *via* computer based image analysis [Optimas, Stemmer, FRG] and the intensity distribution is averaged over one full turn of the sample cell. The software is programmed to account for the slight distortion of the rings due to the cylindrical index match bath.

The distribution of scattered intensity along the Debye-Scherrer ring allows for the determination of texturing in the sample [19]. We define a second angle  $\varphi$  with respect to the  $z$ -axis of the sample cell. Twinned monocrystalline material oriented with its (110) plane parallel to the cell wall gives rise to only six (110) spots at defined values of  $\theta_{B1}$  and  $\varphi$  [19]. The preferred orientation of the [111] direction lies perpendicular to the symmetry axis of the scattering pattern intensity distribution. In addition it is parallel to the formerly applied shear flow. This has been used to decorate the flow pattern of Taylor instabilities in metastable colloidal fluids [10, 17]. For our experiment [111] is directed parallel to the cell axis. In

textured polycrystalline material the (110) Debye-Scherrer ring also shows a sixfold distribution of intensities. A degree of crystallite orientation may be defined by

$$\xi = (I_{6\max} - I_{6\min})/I_{6\max} \quad (6)$$

where  $I_{6\min}$  and  $I_{6\max}$  are the sixfold minimum and maximum intensities. Again the symmetry axis of the intensity distribution is perpendicular to the preferred orientation of [111] crystal directions.

A discrimination between the two morphologies is performed by observing the sample under a given set of  $\Theta_{B_1}$  and  $\varphi$  with a long distance telescopic microscope which gives the spatial distribution of areas scattering under the given Bragg-condition. Wall crystals are conveniently detected and their thickness determined with a resolution better than 20  $\mu$ .

We also observed distributions of intensity showing practically no deviations from complete randomness. These samples containing large numbers of small crystallites were grown directly from the melt at low salt concentrations without further shear processing. We will call these samples unoriented all though a small degree of orientation  $\xi \leq 0.15$  cannot be ruled out in all cases.

Other authors have used rectangular scattering geometries which avoid the distortion of the Debye-Scherrer ring [4, 19]. Then the specular fine structure of single Bragg reflections may be resolved [27]; however no orientational averaging can be performed nor can the scattering vector be changed over a wider range.

Also in our case we may investigate the single reflections seen on one video frame. The form of individual Bragg-spots varies between sharp pointlike ones and more diffuse, broadened along, respectively across the Debye Scherrer ring. In particular at elevated salt concentrations, the latter kind of reflection evolved from the first. This phenomenon appears spontaneously after complete solidification but may also be enforced by the application of low amplitude shear. Recently, similar phenomena have been observed after the ripening of the shear processing of fcc samples [27]. If illuminated by white light, the sample evolves to an overall hazy appearance. If we use the microscope with crossed polarizers twinning indicating by the formation of dark and light stripes is clearly visible [28]. We presently interpret our observation as the relaxation of initially present stress within individual crystals *via* both the straining of other crystals which are orientated more favourably to shearing and the formation of dislocations, respectively as the evolution of stacking faults, i.e. twinning under load.

By shifting the sample in  $z$ -direction we determine the average dimension of crystallites in  $z$ -direction *via* the appearance and disappearance of individual Bragg spots [29]. In samples grown from a shear molten suspension usually round crystals are formed under conditions of homogeneous nucleation [30]. Therefore the dimension in  $z$ -direction is assumed to be equal to the dimensions in  $x$ - and  $y$ -direction. The data recorded this way compare well to those from analysis of microscope video frames.

Thus we have access to the accurate determination of the crystallite size  $\sigma_c$  as well as to local and global orientation of crystallites, which at constant suspension parameters is also highly sensitive to the samples history.

## Results.

**ACCURACY.** — A typical resonance spectrum measured *via*  $\Theta_{B_1}(t)$  is shown in figure 2.  $\omega_{01}$  resonance frequencies are derived considering both peak maxima and phase lag. For all investigated combinations of suspension parameters the  $\omega_{10}$  resonance frequencies from successively taken spectra usually agreed within 1%. The frequencies of higher order resonances are calculated *via* the shear modulus and compared to the experimental values.

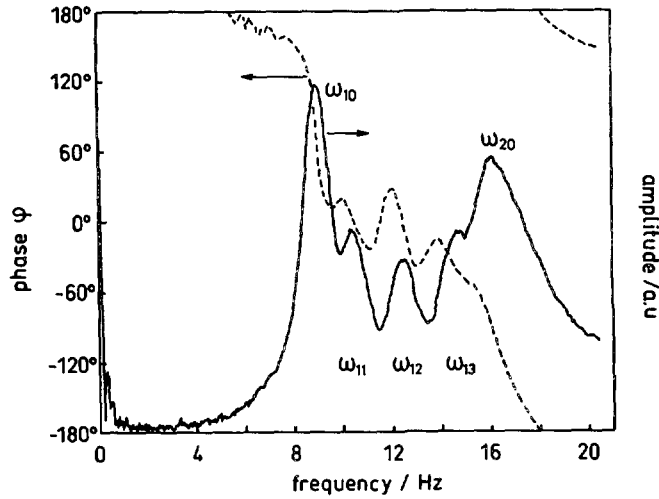


Fig. 2. — Typical resonance spectrum : (—) response amplitude : (---) phase.

Thus usually all higher order peaks can be indexed. Occasional spectra showing agreement to the shear modulus calculated from resonances up to third order not better than 2 % were discarded.

When using the mirror method, only for samples of volume fraction  $\theta \geq 0.04$  the same excellent reproducibility was reached. However, even at the lowest particle concentrations accessible without serious ion contamination problems, the statistical error of the mirror method never exceeded 10 % in  $\omega$ . The mean values of  $\omega$  measured at the same sample coincided for the two methods. This indicates that the mechanical method allows for reasonably accurate checks of elastic sample properties even at low volume fractions, if the suspension parameters are well controlled.

In a polycrystalline sample we usually find crystallites oriented under a given Bragg-conditions at several positions in the cell. Therefore further testing was performed by analysing spectra from i) (110) reflections of crystals at different radial positions in the cell : ii) (110) reflections of crystals at different height and iii) higher order Bragg-reflections. Depending on crystal position higher order resonance frequencies do not always show up with the same amplitude and phase lag. However, within the experimental error of 2 % we find no systematic deviations from the mean value of  $G$ . This result allows for to choose an arbitrary crystal and any Bragg reflection and therefore perform quick and easy but precise measurements.

At large applied amplitudes of excitation the response of the crystals may become nonlinear for two reasons : firstly the harmonic approximation assumed for the interaction potential is only valid for very small elongations and secondly plastic deformations may occur. Therefore we also tested the linearity of the sample's response. With the driving frequency fixed to the  $\omega_{10}$  value we can deduce the distortion of the crystal lattice in dependence on the driving voltage *via* the maximum shift of the Bragg angle. Figure 3 shows the response amplitude of the sample to be linear for driving voltages up to 10 V.

The maximum distortion of the crystal lattice in terms of the nearest neighbour distance never exceeded a few percent and was found to be constant in time for constant driving voltages. For the actual experiments driving voltages between 100 mV and 250 mV were employed corresponding to even smaller distortions on the order of Angströms. We therefore are far from the conditions required for accidental changes in morphology or even shear melting of the sample.

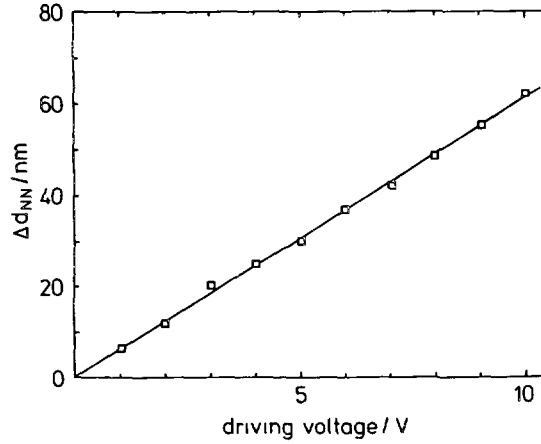


Fig. 3. — Maximum change in nearest neighbour distance  $d_{NN}$  in a bcc unit cell in dependence on the driving voltage.

STABILITY OF THE SUSPENSION PARAMETERS. — One main advantage of the set-up presented here concerns the control of the suspension parameters, in particular the stabilization of the concentration of salt ions and particles. To demonstrate this we compared the evolution of the shear modulus for differently prepared, completely deionized samples of equal particle concentration. All samples were unoriented polycrystalline at the beginning, which appears to be the most stable morphology. The observed decrease in  $G$  was thus attributed to changes in the suspension parameters only. Figure 4 shows a few representative results.

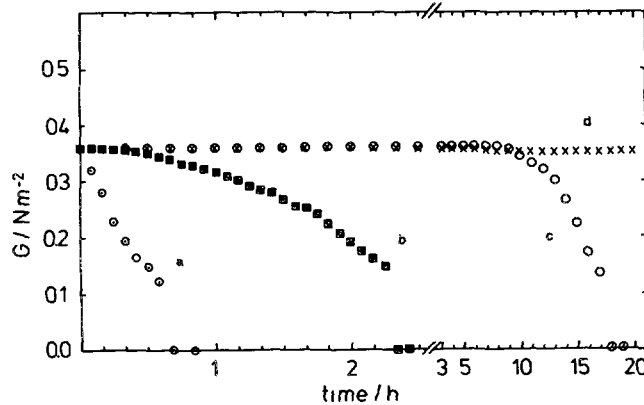


Fig. 4. — Stability of suspension parameters monitored *via* the shear modulus  $G$  for four different preparational techniques. Data are for unoriented polycrystalline samples of  $\Phi \approx 0.0028$  measured by the mirror method a) after CD with free air-suspension interface and ion exchange resin present in the sample cell ; b) after CD with free inert gas-suspension interface but no ion exchange resin present in the sample cell. The other two data sets were recorded by time resolved static light scattering c) after SP with ion exchange resin present but no free suspension surface and optimum sealing and d) after CD with neither ion exchange resin nor a free surface present in the sample cell. Note the change in the time scale for c and d. Compared to the typical duration of a single experiment sufficient stability is obtained for b and excellent results for c and d.

We found that the presence of ion exchange resin in the sample cell inevitably led to gradients in particle concentration. This is consistent with microscopic investigations of the behaviour of charged latices in the vicinity of anion exchanger beads [31]. While working under air, these gradients are seen within some ten minutes after the addition of ion exchange resin and no stable homogeneously crystalline sample could be prepared at all. Instead with SP we most often observed stable gradients in particle concentration leaving the mirror to float freely at the suspension surface [25]. We therefore ion exchanged the suspension by CD and under inert gas but with ion exchange resin present in the measuring cell. The sample behaviour was monitored after the inert gas was replaced by air. According to our present understanding airborne  $\text{CO}_2$  immediately invades the suspension and alters the shear modulus. Once the salt gradients are established, again subsequent gradients in particle concentration are observed. The process is considerably slowed under inert gas atmosphere and acceptable stability is observed. Under cautious handling of inert gas atmosphere and mirror samples are stable for at least the typical duration of an experiment.

Standing preparation with samples completely filled and sealed against air generally yielded stabilities strongly depending on the sealing procedures [25]. Excellent stability was obtained for screw cap plus gas tight membranes covered by the ion exchange resin, where the shear modulus could be stabilized up to several hours. Only after longer times values slightly lower than at the beginning were observed. This however might also be an effect of altered morphology, e.g. less grain boundaries due to ripening processes.

Since the formation of gradients in particle concentration is confined to the vicinity of the ion exchange resin, excellent homogeneity of the suspension is obtained for CD with the ion exchange resin and the free suspension-inert gas surface well separated from the completely filled sample cell. A decrease in  $G$  is only detectable for very long times of  $t \geq 8$  h. when leakage of ions through tube connections starts to become significant. The advantage as compared to tightly sealed standing preparation obviously is the possibility of a systematic variation and control also of the concentration of excess salt.

A number of deionization techniques thus are able to sufficiently stabilize homogeneous suspension parameters in order to ensure reproducible measurements. To realize the goal of monitoring the evolution of the elastic properties over longer periods of e.g. ripening or wearing processes we strongly recommend the absence of a free suspension surface in the sample cell.

### Applications.

**INFLUENCE OF SAMPLE MORPHOLOGY.** — The most important application of our technique lies in the determination of the shear modulus of well characterized samples not only in terms of particle and salt concentration, but moreover in morphology and texture too. Three selected sample morphologies prepared using CD and subsequent shear processing are presented schematically in figure 5.

A) Solidification of a completely shear molten state results in a homogeneously nucleated unoriented polycrystalline material, if heterogeneous nucleation at the cell walls is negligible. This was observed for  $c_s \leq 3 \mu\text{mol l}^{-1}$  at a volume fraction of  $\Phi \approx 0.003$ . The resulting crystals are roughly spherical irregular polygons of approximate diameter  $\sigma_c \approx 0.1$  mm (Fig. 5A).

B) At higher salt concentrations twinned, monolithic crystals heterogeneously nucleated at the cell walls may be grown in addition. These were oriented with their (110) planes parallel to the cell wall and the direction of closest packing, [111], parallel to the formerly applied shear flow, i.e. the  $z$ -axis in figure 1. During the actual shear modulus measurement the probing

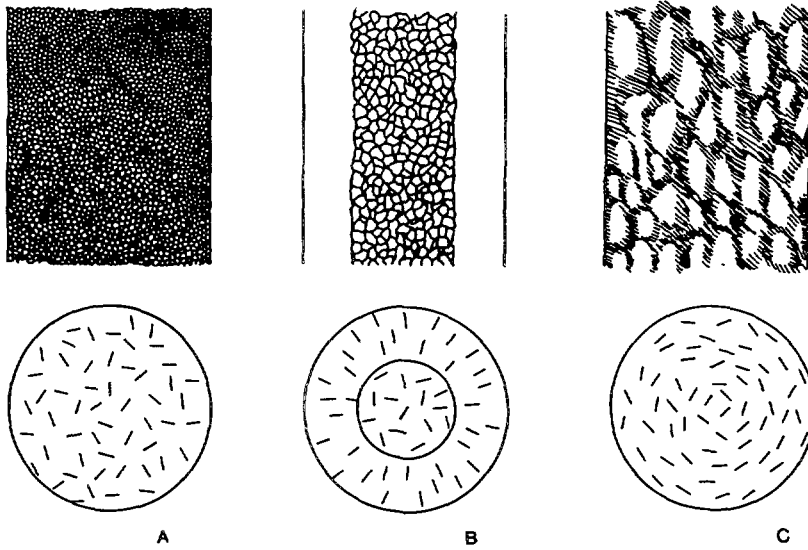


Fig. 5. — Schematic cuts through the sample cell containing colloidal solids of different representative morphologies and preferred orientations. Upper row : vertical cuts showing the approximate size and form of crystallites, respectively grain boundaries ; lower row : horizontal cuts showing schematically the orientation of the  $[111]$  directions. Morphology A : unoriented polycrystalline material with sharp grain boundaries. Morphology B : a twinned monocrystal surrounds a core of unoriented polycrystalline material with sharp grain boundaries. The monocrystal is orientated with its  $(110)$  planes parallel to the cell wall and the direction of closest packing,  $[111]$ , parallel to the formerly applied shear flow. Morphology C : shear processed polycrystalline material showing a noticeable degree of orientation of the  $(110)$  gliding plane with  $[111]$  perpendicular to the cell axis, i.e. parallel to the probe shear direction. Here the grain boundaries are diffuse.

shear oscillation is directed at a right angle to this direction. In a medium range of salt concentrations this wall crystal surrounds a core of unoriented polycrystalline material (Fig. 5B). Both the thickness of the wall crystal and the polycrystal diameters  $\sigma_c$  were found to increase with increasing salt concentration. The maximum size of homogeneously nucleated crystals embedded in the surrounding wall crystal was observed to be roughly 5 mm. Close to the phase boundary the monolithic crystal may fill the whole cell.

C) Samples containing wall crystals were processed further by gentle vertical shearing at rates slightly lower than needed for complete shear melting. This resulted in a semisolid slurry containing bits and pieces of the former wall crystal. It solidificated into a polycrystalline material of non-spherical crystals with typical sizes in the range of  $0.2 \text{ mm} \leq \sigma_c \leq 0.7 \text{ mm}$ , constant with respect to  $c_s$  (Fig. 5C). In this case the grain boundaries appeared hazy or diffuse. We here also found a noticeable degree of orientation of the  $(110)$  gliding plane with  $[111]$  perpendicular to the cell axis, i.e. parallel to the probe shear direction. For the samples shown it increased with increasing  $c_s$  from  $\xi \leq 0.15$  to  $\xi \approx 0.4$ .

Figure 6 presents a compilation of representative results for the three types of morphology. It shows the salt concentration dependence of the shear modulus obtained for a suspension of particle density  $n_p = 3 \times 10^{18} \text{ m}^{-3}$ ; i.e.  $\Phi = 0.0028$ . Since all samples were of bcc structure, the only difference between different samples at equal salt concentration were of morphological and textural nature, as described above. For comparison we include a graph of equation (3) with  $f_A = 0.5$  (unoriented polycrystals). It was fitted to the data of morphology A at  $c_s = 0$  using a constant renormalized charge number of  $Z^* = 395$  as only free parameter. For this value we further calculated the  $c_s$  dependence of  $G$  expected for  $f_A = 0.6$  (homogeneous

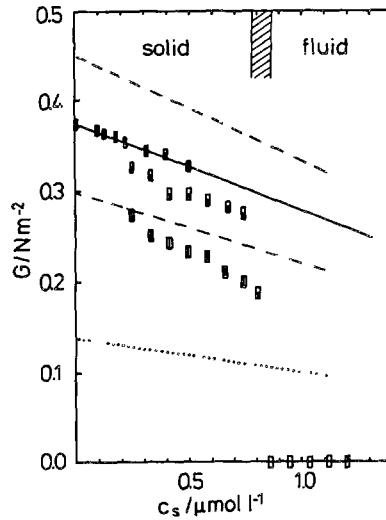


Fig. 6. — Salt concentration dependence of the shear modulus of a suspension of  $\Phi = 0.0028$ . The symbols refer to the experimental data recorded with time resolved static light scattering and the different morphologies (A-C) as shown in figures 5A-C. Filled symbols : unoriented polycrystalline (A) ; half filled symbols : monolithic wall crystal-polycrystalline core (B) ; striped symbols : oriented polycrystalline (C) ; open symbols : fluid samples. The lines refer to theoretical calculations : (—) fit of equation (3) with  $f_A = 0.5$  (unoriented polycrystals) to the data at low salt concentration using a constant renormalized charge number of  $Z^* = 395$  as only fit parameter. (---)  $G$  calculated from that for  $f_A = 0.6$  ; (- · - · -) the same for  $f_A = 0.4$  ; (····) the same for single crystals oriented with [111] parallel to the applied shear. Also included are the observed freezing and melting lines indicating the coexistence region (hatched).

stress),  $f_A = 0.4$  (homogeneous strain) and for single crystalline material completely oriented with its [111] directions parallel to the probing shear.

Morphology A is stable up to  $c_s \approx 0.3 \mu\text{mol l}^{-1}$ . Its shear modulus decreases in accordance with the calculations. The wall crystal-core morphology is stable up to the phase boundary. A discontinuous drop in the shear modulus as compared to morphology A coincides with the appearance of the wall crystal. With increasing salt concentration  $G$  decreases practically parallel to the predictions of equation (3), however, at a considerably lower value. Note that irrespective of the wall crystal's thickness the deviation in  $G$  from the theoretical calculation stays practically constant. At the phase boundary the shear modulus discontinuously drops to zero.

We also include one example of a probe prepared at equilibrium coexistence. The last point for the morphology B was recorded on a sample which was only partially crystallized. It shown a 3 mm thick wall crystal surrounding only few homogeneously nucleated crystallites embedded in colloidal fluid.

The measured shear moduli for the polycrystalline samples oriented with their [111] direction parallel to the probing shear are much lower than the values for morphologies A or B. In particular, they are also lower than the values expected for  $f_A = 0.4$ . While the degree of orientation  $\xi$  of morphology C is increased from  $\xi \leq 0.15$  to  $\xi \approx 0.4$ , the deviation of  $G$  as compared to the predictions of equation (3) further increases. It amounts to a factor of nearly 2 for  $\xi \approx 0.4$ .

The graph clearly shows that with the techniques presented here it is for the first time

possible to unequivocally discriminate between the sometimes very small variations caused by the texture and morphology of crystalline colloidal samples and the overall decrease in  $G$  caused by the addition of salt.

**SYSTEMATIC TESTS OF THEORETICAL DESCRIPTIONS.** — In the last section we have shown that the technique presented here allows for the detection of even slight deviations of the measured shear moduli from the values predicted on the basis of equation (3) and unoriented polycrystalline morphology. Since our method relies on the transparency of the colloidal system, it is ideally suited for measurements at low volume fractions of commercially available charge stabilized particles, in particular as it also provides rigorous control of extremely low salt concentrations. Using particles with nearly matched index of refraction [32] the restriction to low volume fractions of charged spheres falls. The techniques may also be applied to hard sphere systems showing Bragg reflection of visible light [5].

The precise control of experimental parameters, the knowledge of the sample morphology and the accuracy of shear modulus measurements open up the possibility of a wide range of interesting experiments. We would like to shortly discuss three major applications in detail: the test of potential models for charge stabilized samples of defined morphology, the extension of theoretical descriptions of the elastic properties of colloidal solids and the probing of the mutual interdependence of elastic properties and sample behaviour in ripening processes and shear processing.

First of all, the relation between particle data and experimental parameters on one side and the elastic properties on the other side relies on the use of a correct expression for the potential of interaction. The applicability of several potential models for suspensions of highly charged particles at both low volume fraction and salt concentrations has recently been tested [23, 24]. Using the techniques presented here for a shear modulus titration, for the first time the true dissociated charge of the particles was determined *in situ*, i.e. in a crystalline colloidal sample. This true charge of  $Z = 580$  measured at the same conditions reported here was converted to a renormalized charge of  $Z^* = 390$  [22]. It was shown that this charge number used with a Yukawa potential or the modified DLVO approximation (MDA) excellently predicts both elastic and dynamical properties of ordered colloidal suspensions over a wide range of parameters.

In fact, the renormalized charge number derived here from the measurements on morphology A agrees to it within the experimental error. Note however, that this would not be the case for mixed morphologies or in the case of a textured sample.

Secondly, studies on the elastic properties of colloidal crystals do not always show good agreement between theoretical predictions and measured values. This should actually not be due to the preparational methods employed, since both CD and SP give excellent results, if contamination with  $\text{CO}_2$  is excluded.

However, most of the samples investigated so far by other authors were opaque and important information about morphological details was not available. The degree and the direction of preferred orientation of the polycrystalline material was not determined nor was the homogeneity of the sample accessible. Only the outermost regions next to the cell wall were subjected to structural investigations and the samples were assumed to be unoriented polycrystalline. Although our observations show that morphology A is the preferred morphology at deionized conditions and elevated volume fractions, nevertheless a number of other morphological influences exist that may have caused the observed deviations in  $G$  from the expected behaviour.

Equation (3) has been derived under the assumption of unoriented polycrystalline material. It does not include any contribution of inhomogeneity, grain size, grain boundaries, texturing, twinning, dislocations and other imperfections. It is known that with increasingly smaller

volume fraction the size of individual crystallites decreases [29] and may even enter the nanocrystalline regime (less than  $10^9$  particles per crystallite of  $\sigma_c \leq 0.05$  mm). Under these conditions a pronounced influence of the grain size, respectively grain boundary volume on the tracer diffusion coefficient was observed [33]. It would be particularly interesting to monitor the influence of the particle density on the shear modulus, too. With increasing volume of grain boundaries we expect an increasingly homogeneous distribution of stresses and therefore an increase of the averaging factor towards  $f_A = 0.6$ . The same should hold for colloidal glasses.

This would constitute only a first step of an advanced description of elasticity on a microscopic level including morphological details. Further experiments should consider the degree of preferred orientation, the effects of incomplete solidification at equilibrium coexistence, the effects of alloy formation [10, 31] or samples with inhomogeneous morphology or density [25, 26].

Thirdly, such an extended modelling enables the quantitative description also for time dependent measurements which are feasible under conditions of enhanced stability of experimental parameters. Most important information should become available if the shear moduli are measured under shear processing by mechanical [27] or electrical fields [26] and the structural and morphological evolution of the sample is monitored simultaneously by light scattering or microscopic methods. Preliminary experiments on  $G$  during the solidification process should show a percolation transition followed by ripening and orientation processes in the presence of the shearing field.

### Conclusions.

The integration of standard standing preparation (SD) as well as of the recently developed advanced deionization method, — continuous deionization, (CD) [21] — into a novel configuration for the optical detection of resonant shear vibrations was reported. This allowed for a drastic increase in preparational accuracy and sample stability as compared to the former mirror method. Furthermore, using CD in combination with subsequent shear processing, samples of different reproducible morphologies and textures were prepared and characterized extensively by static light scattering.

The precision of the new approach was thoroughly tested and the results were found to be independent of the probed crystallite, its position and orientation within an experimental error of  $\Delta G \leq 2\%$  at absolute values of  $G \approx 0.1 \text{ Nm}^{-2}$ . CD allowed quick and reliable systematic experiments in dependence on the concentration of added neutral electrolyte.

For the first time it became possible to clearly separate the influences of even slightly altered sample morphologies from those of an increased salt concentration.

This allows for high precision tests of charge renormalization theory and of microscopic models for the elasticity of crystalline solids. On the basis of these and on the excellent stability of experimental parameters, new interesting time dependent experiments to probe and describe the mutual interdependence of an individual sample's history on one side and its elastic properties on the other become feasible.

### Acknowledgements.

The authors love to thank M. Würth as well as R. Simon and F. Bitzer for their inspiring comments and their critical remarks on the detection and interpretation of morphological details. H. Löwen is thanked for many helpful discussions on the issue of interaction potentials. We also like to thank R. Beck for her artwork and the referees for their comments on the manuscript. One of us (F.F.) was supported by the European Community within the ERASMUS-program. Last but not least the financial support of the Deutsch Forschungsgemeinschaft is most gratefully acknowledged.

## References

- [1] S. A. Safran, N. A. Clark Eds., *Physics of Complex and Supramolecular Fluids* (N.Y., Wiley-Interscience, 1987).
- [2] Atelier d'Hiver sur les Cristaux Colloïdaux ; Les Houches 1985 : *J. Phys Colloq France* **46** (1985) C3.
- [3] Chen S.-H., Huang J. S., Tartaglia P., *Structure and Dynamics of strongly interacting Colloids and Supramolecular Aggregates*, NATO-ASI vol. **369** (Kluwer, Dordrecht, 1992) p. 39.
- [4] B. J. Ackerson Ed. : *Phase Transitions* **21** (2-4) (1990).
- [5] Pusey P. N., J. P. Hansen, D. Levesque, J. Zinn-Justin Eds., *liquids, freezing and glass transition ; Ecole d'été*, Les Houches 1989, **51** (Amsterdam, Elsevier, 1991) p. 763.
- [6] Crandall R. S., Williams R., *Science* **198** (1977) 293.
- [7] Dubois-Violette E., Pieranski P., Rothen F., Strzlecki L., *J Phys. France* **41** (1980) 369.
- [8] Lindsay H. M., Chaikin P. M., *J. Chem Phys.* **76** (1983) 3774.
- [9] Lindsay H. M., Chaikin P. M., in [2], p. 269.
- [10] Chaikin P. M., di Meglio J. M., Dozier W., Lindsay H. M., Weitz D. A., in [1], p. 65.
- [11] Joanicot M., Jorand M., Pieranski P., Rothen F., *J. Phys France* **45** (1984) 1413.
- [12] Joanny J. F., *J. Coll Interface Sci.* **71** (1979) 622.
- [13] Jorand M., Dubois-Violette E., Pansu B., Rothen F., *J. Phys France* **49** (1988) 1119.
- [14] Robbins M. O., Kremer K., Grest G. S., *J. Chem. Phys.* **88** (1988) 3286.
- [15] Cahn R. W., Haasen R., *Physical Metallurgy* (Amsterdam, Elsevier, 1983).
- [16] Weitz D. A., Dozier W. D., Chaikin P. M., in [2], p. 257.
- [17] Joanicot M., Pieranski P., *J. Phys. Lett. France* **46** (1985) L-91.
- [18] Palberg T., Streicher K., *Nature* **367** (1994) 51.
- [19] Ackerson B. J., *Physica A* **128** (1983) 221.
- [20] Chen L. B., Zukoski C. F., Ackerson B. J., Hanley H. J. M., Straty G. C., Barker J., Glinka C. J., *Phys. Rev Lett* **69** (1992) 688.
- [21] Palberg T., Härtl W., Wittig U., Versmold H., Würth M., Simnacher E., *J. Phys. Chem* **96** (1992) 8180.
- [22] Alexander S., Chaikin P. M., Grant P., Morales G. J., Pincus P., Hone D., *J. Chem Phys* **80** (1984) 5776.
- [23] Palberg T., Kottal J., Bitzer F., Simon R., Würth M., Leiderer P., *J Coll. Interface Sci.* submitted (1993).
- [24] Bitzer F., Palberg T., Lowen H., Simon R., Leiderer P., *Phys. Rev E* submitted (1993).
- [25] Tata B. V. R., Rajalakshmi M., Arora A. K., *Phys. Rev Lett* **69** (1992) 3779 and comment to this paper : Palberg T., Würth M., Simon R., Leiderer P., *Phys Rev Lett* **72** (1994) 786.
- [26] Würth M., Palberg T., *J Chem Phys* submitted (1993).
- [27] Liu J., Weitz D. A., Ackerson B. J., *Phys Rev B* **48** (1993) and Pieranski P., Pansu B. in [2], p. 281.
- [28] Monovoukas Y., Gast A. in [4], p. 183.
- [29] Härtl W., Klemp R., Versmold H., in [4], p. 229.
- [30] Aastuen D. J. W., Clark N. A., Swindal J. C., Muzny C. D., in [4], p. 139.
- [31] Hachisu S., Kobayashi Y., Kose A., *J. Coll. Interface Sci.* **42** (1973) 342.
- [32] Piazza R., Degiorgio V., *Physica A* **182** (1992) 576.
- [33] Simon R., Palberg T., Leiderer P., *J Chem. Phys* **99** (1993) 3030.